# Wireless Energy-Harvesting Cognitive Radio with Feature Detectors

**Yan Gao[1], Yunfei Chen[2], Zhibin Xie[3] and Guobing Hu[4]**
[1] School of Electronic Information, Nanjing College of Information Technology, Nanjing, China
[e-mail: gaoyan@njcit.cn]
[2] School of Engineering, Warwick University
Coventry, CV4 7AL, UK
[e-mail: yunfei.chen@warwick.ac.uk]
[3]School of Electronic and Information, Jiangsu University of Science and Technology, Zhenjiang, China
[e-mail: xiezhibin@just.edu.cn]
[4]School of Electronic Information Engineering, Jinling Institute of Technology, Nanjing, China
[e-mail: hugb@njcit.cn]
*Corresponding author: Yunfei Chen

---

## *Abstract*

The performances of two commonly used feature detectors for wireless energy-harvesting cognitive radio systems are compared with the energy detector under energy causality and collision constraints. The optimal sensing duration is obtained by analyzing the effect of the detection threshold on the average throughput and collision probability. Numerical examples show that the covariance detector has the optimal sensing duration depending on an appropriate choice of the detection threshold, but no optimal sensing duration exists for the ratio of average energy to minimum eigenvalue detector.

---

## 1. Introduction

**E**nergy-harvesting is a promising solution to green communications [1], [2]. For example, it can be used in future networks by harvesting energy from both ambient sources or licensed users [3]. It can be used to harvest energy along with interference alignment [4], [5]. It can also be used to provide energy for cognitive relaying [6]. Recently, much research work has focused on energy-harvesting in cognitive radio networks(CRNs) harvesting from ambient sources only [7]-[10]. In particular, researchers have studied the effects of different sensing parameters, such as sensing duration, sensing threshold and transmit power on the system performance. In [7] and their other works, the spectrum sensing policy and the detection threshold for an energy harvesting CR were jointly designed under the energy causality and collision constraints to maximize the expected total throughput. In [8], the optimal transmit power was studied jointly with the sensing duration and sensing threshold to maximize the average throughput. In [9], optimal and myopic sensing strategies are studied based on the proposed channel selection criterion under energy neutrality constraint and fading channel conditions. In [10], optimal sensing and access policies are analyzed in energyharvesting CR for a single-user single-channel setting in the presence of sensing errors. However, all the aforementioned works have studied energy detector only.

Energy detection is known for its simplicity but also for its poor performance due to various factors, such as noise uncertainty [11]. Consequently, feature detection is commonly used for spectrum sensing. In [12], a maximum eigenvalue (ME) detector based on the statistical covariance of the received signal was shown to have a better performance than the energy detector for correlated signals. In [13], the ratio of maximum to minimum eigenvalue(MME) and the ratio of average energy to minimum eigenvalue (EME) detector were proposed. In [14], a covariance(COV) detector was proposed to outperform the energy detector. In [15], the four feature detectors discussed above were compared with primary user traffic during the sensing period. All these feature detectors provide useful alternatives to the energy detector. However, their use in energy-harvesting cognitive radio systems has not been studied yet.

In this paper, we investigate the use of feature detectors in energy-harvesting cognitive radio systems harvesting from ambient sources only and compare their performances with that using energy detection. Due to different detection variables and detection thresholds used in feature detection and energy detection, the effects of some sensing parameters, as studied in [7]-[10], will be added or removed. Numerical results give insights into the effect of the different sensing thresholds on the system performance and how to design the sensing duration for a given detection threshold in an energy-harvesting CRN. A list of important variables and symbols in this paper are presented in **Table 1** for readers' convenience.

**Table 1.** List of important variables and symbols used in the paper.

| COV | Covariance detector |
|-----|---------------------|
| EG  | Energy detector |
| EME | Average-energy-to-minimum-eigenvalue detector |

| ST | Secondary transmitter |
|---|---|
| $a_t$ | Spectrum access mode |
| $E_t$ | Residual energy at time t |
| $E_t^c$ | Consumed energy at time t |
| $E_t^h$ | Harvested energy at time t |
| $e_h$ | Average harvested energy |
| $e_s$ | Sensing energy |
| $e_t$ | Transmitting energy |
| $f_s$ | Sampling frequency |
| $p_s$ | Sensing power |
| $p_t$ | Transmission power |
| $P_D$ | Detection probability |
| $P_{FA}$ | False alarm probability |
| $P_a$ | Active probability |
| $P_v$ | Availability probability |
| $P_c$ | Collision probability |
| $R$ | Average throughput |
| $R_u$ | Average throughput of energy unconstrained CR |
| $SNR_p$ | Signal-to-noise ratio of primary user |
| $SNR_s$ | Signal-to-noise ratio of secondary user |
| $T$ | Time slot length |
| $\theta_t$ | Sensing decision or result |
| $\gamma$ | Detection threshold |
| $\tau_s$ | Sensing duration |
| $\tau_c$ | Minimum feasible sensing duration |
| $\tau_e$ | Minimum energy equilibrium sensing duration |
| $\tau_p$ | Optimal sensing duration |
| $\pi_0, \pi_1$ | Idle and occupancy probabilities |

## 2. System Model

Consider a CRN model comprising of a primary user and an energy-harvesting secondary network. The primary user is licensed to utilize the spectrum, while the secondary network opportunistically accesses the primary user's spectrum.Assume that there is no fixed energy supply for the secondary users, such that it collects energy from ambient sources(e.g., solar, wind, vibration, ambient radio frequency) for spectrum sensing and data transmission.

### 2.1 Energy Model and Spectrum Access Decision

The energy-harvesting secondary transmitter(ST) will be either active or inactive, depending on the residual energy $E_t$ at the beginning of slot $t$. Suppose that the duration of each slot $T$ is divided into a sensing time of $\tau_s$ and a data transmission time of $T - \tau_s$. Assume the ST always has data to transmit. Define $\tau_s / T$ as the normalized sensing duration, which is the ratio of the sensing duration to the total slot duration. Denote $E_t^h > 0$ as the harvested energy at slot $t$, which is assumed to be an independent and identically distributed random process with mean $E\{E_t^h\} = e_h$. The required energy per slot for spectrum sensing and data transmission are $e_s = p_s \tau_s$ and $e_t = p_t(T - \tau_s)$, respectively, where $p_s > 0$ is the sensing power and $p_t > 0$ is the transmission power. If the residual energy $E_t$ is greater than or equal to $e_s + e_t$, the ST performs spectrum sensing and data transmission during slot $t$. Otherwise, it will not be active. Denote $a_t = \{0(inactive), 1(active)\}$ as the spectrum access mode, a decision made by ST as

$$a_t = \begin{cases} 1, & E_t \geq e_s + e_t \\ 0, & E_t < e_s + e_t \end{cases}. \tag{1}$$

When $a_t = 0$ (ST is in the inactive mode), the ST takes no action and turns off itself until the next slot arrives. When $a_t = 1$ (ST is in the active mode), the ST carries out spectrum sensing with $e_s$ energy consumption. Based on the sensing result $\theta_t = \{0(idle), 1(occupied)\}$, the ST decides whether it will transmit data or not. When $\theta_t = 0$ (the spectrum is idle), the ST consumes $e_t$ for data transmission. Otherwise, when $\theta_t = 1$ (the spectrum is occupied), the ST does not take any action. The total consumed energy of ST in a slot $t$ is $E_t^c = a_t(e_s + (1 - \theta_t)e_t)$ and the residual energy at the beginning of the next slot $t + 1$ is $E_{t+1} = E_t - E_t^c + E_t^h$.

### 2.2 Spectrum Sensing

The ST carries out spectrum sensing in the active mode. The probabilities of an idle or occupied band are denoted by $\pi_0$ and $\pi_1$, respectively, with $\pi_0 + \pi_1 = 1$. The binary hypothesis test for spectrum sensing is

$$\begin{aligned} H_0 &: y_t(m) = w_t(m) \\ H_1 &: y_t(m) = s_t(m) + w_t(m) \end{aligned}. \tag{2}$$

where $y_t(m)$ is the $m$-th sample of the received signal in slot $t$, $s_t(m)$ and $w_t(m)$ are the primary user signal and noise, respectively, assumed to be real-valued zero-mean Gaussian

random variables with variances $\sigma_p^2$ and $\sigma_w^2$, respectively. Denote $f_s$ as the sampling frequency. Then, the number of samples is $N = \tau_s f_s$. The ST detects the presence of the primary signal using different detectors. Their probabilities of false alarm and detection under two hypotheses are discussed as follows.

For energy detector (EG), the probability of false alarm $P_{FA}^{EG}$ and the probability of detection $P_D^{EG}$ were derived as

$$P_{FA}^{EG}(\tau_s, \gamma_{EG}) \approx Q\left((\gamma_{EG} - 1)\sqrt{\frac{\tau_s f_s}{2}}\right) \qquad (3).$$

$$P_D^{EG}(\tau_s, \gamma_{EG}) \approx Q\left((\frac{\gamma_{EG}}{SNR_p + 1} - 1)\sqrt{\frac{\tau_s f_s}{2}}\right) \qquad (4)$$

respectively, where $\gamma_{EG}$ is the detection threshold, $SNR_p = \sigma_p^2 / \sigma_w^2$ is the received signal-to-noise ratio(SNR) of the primary user, $Q(x) = \frac{1}{\sqrt{2\pi}}\int_x^{+\infty} e^{-u^2/2} du$ is the Gaussian $Q$ function.

For the EME detector, the probability of false alarm $P_{FA}^{EME}$ and the probability of detection $P_D^{EME}$ are given by

$$P_{FA}^{EME}(\tau_s, \gamma_{EME}) \approx Q\left(\frac{\gamma_{EME}(\sqrt{\tau_s f_s} - \sqrt{L})^2 - \tau_s f_s}{\sqrt{2\tau_s f_s}}\right) \qquad (5)$$

$$P_D^{EME}(\tau_s, \gamma_{EME}) \approx Q\left(\frac{\gamma_{EME}\left(\rho_{\min} + \frac{\sigma_w^2}{\sqrt{\tau_s f_s}}(\sqrt{\tau_s f_s} - \sqrt{L})\right) - \frac{T_r(R_s)}{L} - \sigma_w^2}{\sqrt{\frac{2}{\tau_s f_s}}\sigma_w^2}\right) \qquad (6)$$

respectively, where $\gamma_{EME}$ is the detection threshold, $L$ is the smoothing factor, $\bar{R}_s$ is the covariance matrix of $s(m)$, $\rho_{\min}$ is the minimum eigenvalues of $\bar{R}_s$ and $T_r(R_s)$ is the trace of $\bar{R}_s$.

For the COV detector, the probability of false alarm $P_{FA}^{COV}$ and the probability of detection $P_D^{COV}$ are given by

$$P_{FA}^{COV}(\tau_s, \gamma_{COV}) \approx 1 - Q\left(\frac{\frac{1}{\gamma_{COV}}\left(1 + (L-1)\sqrt{\frac{2}{\tau_s f_s \pi}}\right) - 1)}{\sqrt{\frac{2}{\tau_s f_s}}}\right) \qquad (7)$$

$$P_D^{COV}(\tau_s, \gamma_{COV}) \approx 1 - Q\left(\frac{\frac{1}{\gamma_{COV}} + \frac{\gamma_L \sigma_p^2}{\gamma_{COV}(\sigma_p^2 + \sigma_w^2)} - 1}{\sqrt{\frac{2}{\tau_s f_s}}}\right) \qquad (8)$$

respectively, where $\gamma_{COV}$ is the detection threshold and $\gamma_L = (2/L)\sum_{l=0}^{L-1}(L-l)\left|E[s(m)s(m-l)]/\sigma_p^2\right|$.

Next, we derive the performances of energy harvesting CRNs using these detectors.

# 3. Performance Comparison

The aim of the ST is to transmit data successfully under the energy causality constraint, while the probability of collision should be below a target probability to guarantee the QoS of primary user. From the discussion above, it is shown that the sensing duration depends on the spectrum access mode decision and spectrum sensing performance. Thus, its effect on system performance needs to be investigated further.

## 3.1 Active Probability

Consider the fact that the active probability is limited by the energy causality constraint. Thus, the harvested energy should be no less than the consumed energy. Otherwise, the average throughput will be degraded when ST enters into the inactive mode.

The active probability for EG can be derived as

$$P_a^{\text{EG}}(\tau_s, \gamma_{\text{EG}}, e_h) = \min(1, \lambda_{\text{EG}}(\tau_s, \gamma_{\text{EG}}, e_h)) \tag{9}$$

$$\lambda_{\text{EG}}(\tau_s, \gamma_{\text{EG}}, e_h) = \frac{e_h}{p_s \tau_s + p_t(T - \tau_s)\{(1 - P_{FA}^{\text{EG}}(\tau_s, \gamma_{\text{EG}}))\pi_0 + (1 - P_D^{\text{EG}}(\tau_s, \gamma_{\text{EG}}))\pi_1\}} \tag{10}$$

being the ratio of the average harvested energy to the average energy consumption.

We can see that the harvested energy is independent of $\tau_s$ while the consumed energy depends on $\tau_s$. Thus, for a given $e_h$, according to $\lambda_{\text{EG}}(\tau_s, \gamma_{\text{EG}}, e_h)$, there exists three operating regions of ST as follows:

a)  The system operates in energy-surplus region: $\lambda_{\text{EG}}(\tau_s, \gamma_{\text{EG}}, e_h) > 1$. The set of sensing durations in this region is $T_s = \{\tau | \lambda_{\text{EG}}(\tau_s, \gamma_{\text{EG}}, e_h) > 1\}$.

b)  The system operates in the energy-equilibrium region: $\lambda_{\text{EG}}(\tau_s, \gamma_{\text{EG}}, e_h) = 1$. The set of sensing durations in this region is $T_e = \{\tau | \lambda_{\text{EG}}(\tau_s, \gamma_{\text{EG}}, e_h) = 1\}$.

c)  The system operates in the energy-deficit region: $\lambda_{\text{EG}}(\tau_s, \gamma_{\text{EG}}, e_h) < 1$. The set of sensing durations in this region is $T_d = \{\tau | \lambda_{\text{EG}}(\tau_s, \gamma_{\text{EG}}, e_h) < 1\}$.

When $\lambda_{\text{EG}}(\tau_s, \gamma_{\text{EG}}, e_h) > 1$, the average harvested energy is greater than consumed energy, $P_a^{\text{EG}}(\tau_s, \gamma_{\text{EG}}, e_h) = 1$. This means that the system always executes opportunistic spectrum access, since it has enough energy for spectrum access. On the other hand, when $\lambda_{\text{EG}}(\tau_s, \gamma_{\text{EG}}, e_h) < 1$, $P_a^{\text{EG}}(\tau_s, \gamma_{\text{EG}}, e_h) = \lambda_{\text{EG}}(\tau_s, \gamma_{\text{EG}}, e_h)$, which means the ST should stay in the inactive mode and suffers from energy shortage for most time slots. When $\lambda_{\text{EG}}(\tau_s, \gamma_{\text{EG}}, e_h) = 1$, the ST is consuming as much energy as what it has harvested on average, so it remains in active mode all the time. For the EME and COV detectors, there are also three operating regions of ST with similar characteristics as EG by replacing the subscript 'EG' with 'EME' and 'COV', respectively, in the $\lambda_{\text{EG}}(\tau_s, \gamma_{\text{EG}}, e_h)$.

## 3.2 Availability and Collision Probability

Compared with energy-unconstrained CRN, the performances of the energy-harvesting CR system are affected by the energy causality constraint and spectrum sensing performance. This means that we have to define new performance metrics, namely, the availability probability and the collision probability.

The probability that the ST accesses the idle spectrum and can transmit data without interference is called the availability probability. The probability that the ST accesses the occupied spectrum and its signal will be colliding with the primary signal is called the collision probability.

For EG, the availability probability can be expressed as

$$P_v^{\text{EG}}(\tau_s, \gamma_{\text{EG}}, e_h) = P_a^{\text{EG}}(\tau_s, \gamma_{\text{EG}}, e_h)(1 - P_{FA}^{\text{EG}}(\tau_s, \gamma_{\text{EG}})) \quad (11)$$

Also, the collision probability for EG is given by

$$P_c^{\text{EG}}(\tau_s, \gamma_{\text{EG}}, e_h) = P_a^{\text{EG}}(\tau_s, \gamma_{\text{EG}}, e_h)(1 - P_D^{\text{EG}}(\tau_s, \gamma_{\text{EG}})) \quad (12)$$

Using similar methods, one can have these probabilities for the EME and COV detectors as

$$P_a^{\text{EME}}(\tau_s, \gamma_{\text{EME}}, e_h) = \min(1, \lambda_{\text{EME}}(\tau_s, \gamma_{\text{EME}}, e_h)) \quad (13)$$

where

$$\lambda_{\text{EME}}(\tau_s, \gamma_{\text{EME}}, e_h) = \frac{e_h}{p_s \tau_s + p_t(T - \tau_s)\{(1 - P_{FA}^{\text{EME}}(\tau_s, \gamma_{\text{EME}}))\pi_0 + (1 - P_D^{\text{EME}}(\tau_s, \gamma_{\text{EME}}))\pi_1\}} \quad (14)$$

$$P_v^{\text{EME}}(\tau_s, \gamma_{\text{EME}}, e_h) = P_a^{\text{EME}}(\tau_s, \gamma_{\text{EME}}, e_h)(1 - P_{FA}^{\text{EME}}(\tau_s, \gamma_{\text{EME}})) \quad (15)$$

$$P_c^{\text{EME}}(\tau_s, \gamma_{\text{EME}}, e_h) = P_a^{\text{EME}}(\tau_s, \gamma_{\text{EME}}, e_h)(1 - P_D^{\text{EME}}(\tau_s, \gamma_{\text{EME}})) \quad (16)$$

$$P_a^{\text{COV}}(\tau_s, \gamma_{\text{COV}}, e_h) = \min(1, \lambda_{\text{COV}}(\tau_s, \gamma_{\text{COV}}, e_h)) \quad (17)$$

where

$$\lambda_{\text{COV}}(\tau_s, \gamma_{\text{COV}}, e_h) = \frac{e_h}{p_s \tau_s + p_t(T - \tau_s)\{(1 - P_{FA}^{\text{COV}}(\tau_s, \gamma_{\text{COV}}))\pi_0 + (1 - P_D^{\text{COV}}(\tau_s, \gamma_{\text{COV}}))\pi_1\}} \quad (18)$$

$$P_v^{\text{COV}}(\tau_s, \gamma_{\text{COV}}, e_h) = P_a^{\text{COV}}(\tau_s, \gamma_{\text{COV}}, e_h)(1 - P_{FA}^{\text{COV}}(\tau_s, \gamma_{\text{COV}})) \quad (19)$$

$$P_c^{\text{COV}}(\tau_s, \gamma_{\text{COV}}, e_h) = P_a^{\text{COV}}(\tau_s, \gamma_{\text{COV}}, e_h)(1 - P_D^{\text{COV}}(\tau_s, \gamma_{\text{COV}})). \quad (20)$$

## 3.3 Average throughput

In the energy-harvesting CR system, the average throughput for EG can be expressed as

$$R_{\text{EG}}(\tau_s, \gamma_{\text{EG}}, e_h) = P_a^{\text{EG}}(\tau_s, \gamma_{\text{EG}}, e_h) R_u^{\text{EG}}(\tau_s, \gamma_{\text{EG}}) \quad (21)$$

$$R_u^{\text{EG}}(\tau_s, \gamma_{\text{EG}}) = \frac{T - \tau_s}{T}((1 - P_{FA}^{\text{EG}}(\tau_s, \gamma_{\text{EG}}))\pi_0 + (1 - P_D^{\text{EG}}(\tau_s, \gamma_{\text{EG}}))\pi_1)C_0 \quad (22)$$

refers to the average throughput of an energy-unconstrained CRN, $C_0 = \log(1 + SNR_s)$ and $SNR_s$ indicates the secondary *SNR*.

For the EME and COV detectors, their average throughputs can be obtained by using the similar methods as

$$R_{\text{EME}}(\tau_s, \gamma_{\text{EME}}, e_h) = P_a^{\text{EME}}(\tau_s, \gamma_{\text{EME}}, e_h) R_u^{\text{EME}}(\tau_s, \gamma_{\text{EME}}) \tag{23}$$

$$R_u^{\text{EME}}(\tau_s, \gamma_{\text{EME}}) = \frac{T - \tau_s}{T}((1 - P_{FA}^{\text{EME}}(\tau_s, \gamma_{\text{EME}}))\pi_0 + (1 - P_D^{\text{EME}}(\tau_s, \gamma_{\text{EME}}))\pi_1)C_0 \tag{24}$$

$$R_{\text{COV}}(\tau_s, \gamma_{\text{COV}}, e_h) = P_a^{\text{COV}}(\tau_s, \gamma_{\text{COV}}, e_h) R_u^{\text{COV}}(\tau_s, \gamma_{\text{COV}}) \tag{25}$$

$$R_u^{\text{COV}}(\tau_s, \gamma_{\text{COV}}) = \frac{T - \tau_s}{T}((1 - P_{FA}^{\text{COV}}(\tau_s, \gamma_{\text{COV}}))\pi_0 + (1 - P_D^{\text{COV}}(\tau_s, \gamma_{\text{COV}}))\pi_1)C_0 . \tag{26}$$

## 4. Optimal sensing duration policy

In order to maximize the average throughput of energy harvesting CR system, the optimal sensing duration needs to be designed under energy causality constraint and the collision constraint simultaneously. The derivation can be obtained following the method in [7] – [10] and therefore is not presented here to focus on the discussion instead.

### 4.1 Minimum Feasible Sensing Duration under Collision Constraint

The minimum feasible sensing duration, denoted as $\tau_c^{\text{EG}}(\gamma_{\text{EG}}, e_h)$ for EG, is the minimum boundary element of a feasible set that satisfies the equality of the collision constraint and can be given by

$$\tau_c^{\text{EG}}(\gamma_{\text{EG}}, e_h) = \begin{cases} 0, & \overline{P}_c > \max\limits_{\tau_s}\left\{P_c^{\text{EG}}(\tau_s, \gamma_{\text{EG}}, e_h)\right\} \\ \{\phi\}, & \overline{P}_c < \min\limits_{\tau_s}\left\{P_c^{\text{EG}}(\tau_s, \gamma_{\text{EG}}, e_h)\right\} \\ P_c^{-1}(\overline{P}_c, \gamma_{\text{EG}}, e_h), & otherwise \end{cases} \tag{27}$$

where $P_c^{-1}(\cdot, \gamma_{\text{EG}}, e_h)$ is the inverse of $P_c(\cdot, \gamma_{\text{EG}}, e_h)$ and $\overline{P}_c$ is the target collision probability.

For the EME and COV detectors, their definitions can be obtained by

$$\tau_c^{\text{EME}}(\gamma_{\text{EME}}, e_h) = \begin{cases} 0, & \overline{P}_c > \max\limits_{\tau_s}\left\{P_c^{\text{EME}}(\tau_s, \gamma_{\text{EME}}, e_h)\right\} \\ \{\phi\}, & \overline{P}_c < \min\limits_{\tau_s}\left\{P_c^{\text{EME}}(\tau_s, \gamma_{\text{EME}}, e_h)\right\} \\ P_c^{-1}(\overline{P}_c, \gamma_{\text{EME}}, e_h), & otherwise \end{cases} \tag{28}$$

where $P_c^{-1}(\cdot, \gamma_{\text{EME}}, e_h)$ is the inverse of $P_c(\cdot, \gamma_{\text{EME}}, e_h)$ and $\overline{P}_c$ is the target collision probability.

$$\tau_c^{\mathrm{COV}}(\gamma_{\mathrm{COV}},e_h) = \begin{cases} 0, & \bar{P}_c > \max_{\tau_s}\left\{P_c^{\mathrm{COV}}(\tau_s,\gamma_{\mathrm{COV}},e_h)\right\} \\ \{\phi\}, & \bar{P}_c < \min_{\tau_s}\left\{P_c^{\mathrm{COV}}(\tau_s,\gamma_{\mathrm{COV}},e_h)\right\} \\ P_c^{-1}(\bar{P}_c,\gamma_{\mathrm{COV}},e_h), & otherwise \end{cases} \tag{29}$$

where $P_c^{-1}(\cdot,\gamma_{\mathrm{COV}},e_h)$ is the inverse of $P_c(\cdot,\gamma_{\mathrm{COV}},e_h)$ and $\bar{P}_c$ is the target collision probability.

## 4.2 Minimum Energy-Equilibrium Sensing Duration under Energy Causality Constraint

It is worth noting that the average throughput is degrading with the sensing duration in energy-deficit region. So the sensing duration should be adjusted to the energy-equilibrium region in order to avoid performance degradation. The minimum energy equilibrium sensing duration, denoted as $\tau_e^{\mathrm{EG}}(\gamma_{\mathrm{EG}},e_h)$ for EG, is the minimum element of the energy-equilibrium set larger than or equal to $\tau_c^{\mathrm{EG}}(\gamma_{\mathrm{EG}},e_h)$. It is derived as

$$\tau_e^{\mathrm{EG}}(\gamma_{\mathrm{EG}},e_h) = \min\left\{1_{\left\{\lambda_{\mathrm{EG}}^{-1}(1,\gamma_{\mathrm{EG}},e_h)>\tau_c^{\mathrm{EG}}(\gamma_{\mathrm{EG}},e_h)\right\}}\lambda_{\mathrm{EG}}^{-1}(1,\gamma_{\mathrm{EG}},e_h)\right\} \tag{30}$$

where $\lambda_{\mathrm{EG}}^{-1}(\cdot,\gamma_{\mathrm{EG}},e_h)$ is the inverse of $\lambda_{\mathrm{EG}}(\cdot,\gamma_{\mathrm{EG}},e_h)$ and $\tau_c^{\mathrm{EG}}(\gamma_{\mathrm{EG}},e_h)$ is denoted in (27).

For the EME and COV detectors, their definitions can be derived by

$$\tau_e^{\mathrm{EME}}(\gamma_{\mathrm{EME}},e_h) = \min\left\{1_{\left\{\lambda_{\mathrm{EME}}^{-1}(1,\gamma_{\mathrm{EME}},e_h)>\tau_c^{\mathrm{EME}}(\gamma_{\mathrm{EME}},e_h)\right\}}\lambda_{\mathrm{EME}}^{-1}(1,\gamma_{\mathrm{EME}},e_h)\right\} \tag{31}$$

where $\lambda_{\mathrm{EME}}^{-1}(\cdot,\gamma_{\mathrm{EME}},e_h)$ is the inverse of $\lambda_{\mathrm{EME}}(\cdot,\gamma_{\mathrm{EME}},e_h)$ and $\tau_c^{\mathrm{EME}}(\gamma_{\mathrm{EME}},e_h)$ is denoted in (28).

$$\tau_e^{\mathrm{COV}}(\gamma_{\mathrm{COV}},e_h) = \min\left\{1_{\left\{\lambda_{\mathrm{COV}}^{-1}(1,\gamma_{\mathrm{COV}},e_h)>\tau_c^{\mathrm{COV}}(\gamma_{\mathrm{COV}},e_h)\right\}}\lambda_{\mathrm{COV}}^{-1}(1,\gamma_{\mathrm{COV}},e_h)\right\} \tag{32}$$

where $\lambda_{\mathrm{COV}}^{-1}(\cdot,\gamma_{\mathrm{COV}},e_h)$ is the inverse of $\lambda_{\mathrm{COV}}(\cdot,\gamma_{\mathrm{COV}},e_h)$ and $\tau_c^{\mathrm{COV}}(\gamma_{\mathrm{COV}},e_h)$ is denoted in (29).

## 4.3 Solution to Optimization Problem for Throughput Maximization

Combining the discussions in parts *4.1* and *4.2*, the candidate for the solution of sensing duration for EG is $\tau_c^{\mathrm{EG}}(\gamma_{\mathrm{EG}},e_h) \le \tau_s \le \tau_e^{\mathrm{EG}}(\gamma_{\mathrm{EG}},e_h)$. If this solution belongs to $T_d$, the optimal duration is set to $\tau_c^{\mathrm{EG}}(\gamma_{\mathrm{EG}},e_h)$ so that the average throughput will not decrease. Otherwise, the sensing-throughput tradeoff should be considered jointly. In fact, there exists a maximum point $\tau_m^{\mathrm{EG}}(\gamma_{\mathrm{EG}},e_h)$ of $R_u^{\mathrm{EG}}(\tau_s,\gamma_{\mathrm{EG}})$ from the tradeoff. This $\tau_m^{\mathrm{EG}}(\gamma_{\mathrm{EG}},e_h)$ does not vary with $e_h$ and satisfies the sensing duration that maximizes $R_u^{\mathrm{EG}}(\tau_s,\gamma_{\mathrm{EG}})$ in energy-unconstrained CRN, i.e., $\dfrac{\partial R_u^{\mathrm{EG}}(\tau_s,\gamma_{\mathrm{EG}})}{\partial \tau_s} = 0$. Consequently, the optimal sensing duration is determined by comparing three candidates, $\tau_c^{\mathrm{EG}}(\gamma_{\mathrm{EG}},e_h)$, $\tau_m^{\mathrm{EG}}(\gamma_{\mathrm{EG}},e_h)$ and $\tau_e^{\mathrm{EG}}(\gamma_{\mathrm{EG}},e_h)$ to achieve the average throughput

maximization.

Thus, for a given sensing threshold, the general expression of optimal sensing duration $\tau_p^{\text{EG}}(\gamma_{\text{EG}}, e_h)$ for EG can be derived as

$$\tau_p^{\text{EG}}(\gamma_{\text{EG}}, e_h) = \underset{\tau \in \left\{ \tau_c^{\text{EG}}(\gamma_{\text{EG}}, e_h), \tau_m^{\text{EG}}(\gamma_{\text{EG}}, e_h), \tau_e^{\text{EG}}(\gamma_{\text{EG}}, e_h) \right\}}{\arg \max} R_{\text{EG}}(\tau_s, \gamma_{\text{EG}}, e_h) \qquad (33)$$

The optimal sensing durations for EME and COV detectors are found in a similar way by replacing "EG" in (33) with "EME" and "COV", respectively. They are not repeated here to save space. Their optimal solutions will be discussed in the next section.

## 5. Numerical results and discussion

In this section, the performances of the feature detectors are compared with the energy detector for energy-harvesting CRN. The system parameters used in the comparison are summarized in **Table 2**. The smoothing factor is chosen to 8 as in [15]. It was shown in the feature detection literature that a larger $L$ gives better performance but more complicated detector. Furthermore, since the COV and EME detectors cannot have the sensing duration as 0, we set $\tau_s$ to $[T_1, T]$, where $T_1 = 0.001$ is non-zero in our simulation.

**Table 2.** SIMULATION PARAMETERS

| Symbol | Description | Value |
|--------|-------------|-------|
| $p_s$ | Sensing power | 110mW |
| $p_t$ | Transmit power | 410mW |
| $\pi_0$ | Probability of being idle | 0.8 |
| $\sigma_w^2$ | Noise power | 1 |
| $SNR_\rho$ | Primary signal SNR | -15dB |
| $SNR_S$ | Secondary SNR | 20dB |
| $f_s$ | Sampling frequency | 1MHz |
| $T$ | Slot duration | 0.1s |
| $\bar{P}_c$ | Target collision probability | 0.1 |
| $L$ | Smoothing factor | 8 |

**Figs. 1** and **2** compare the average energy consumption versus the normalized sensing duration for the EG and COV detectors with different detection thresholds. **Fig. 1** indicates the average energy consumption for EG when $\gamma_{\text{EG}} = 1.005 \sim 1.01$ from the bottom to the top, and **Fig. 2** shows for COV when $\gamma_{\text{COV}} = 1.02 \sim 1.025$ from the bottom to the top.
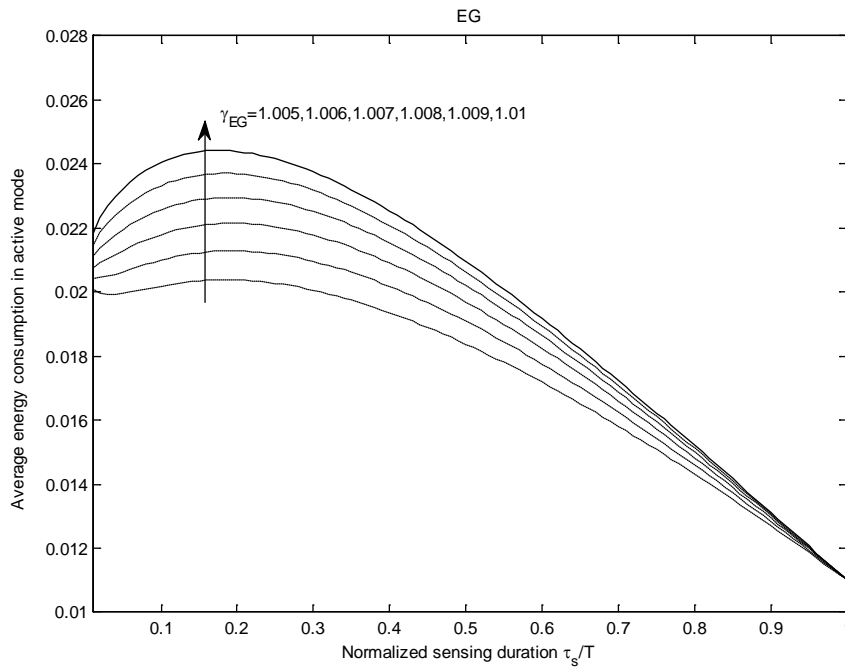
**Fig. 1.** Average energy consumption versus the normalized sensing duration for energy detector with various detection thresholds.
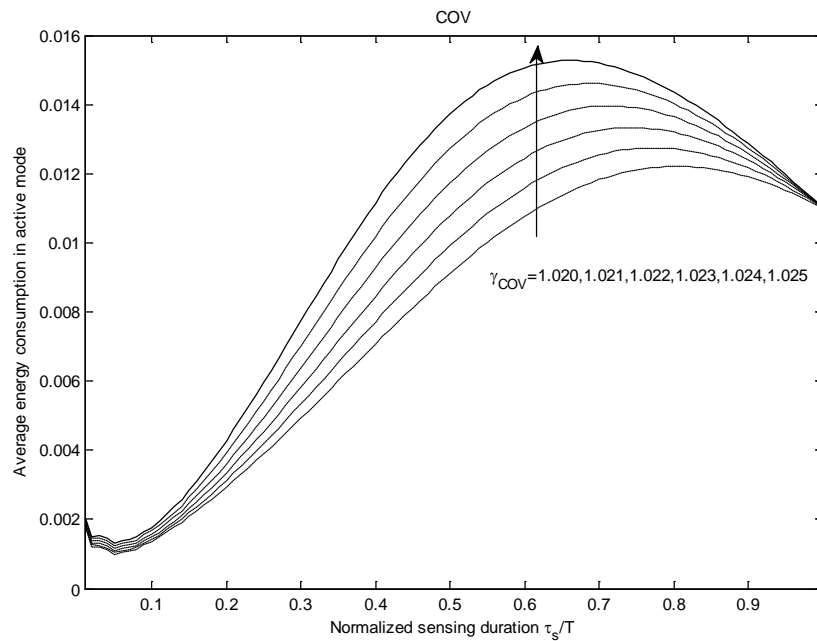


**Fig. 2.** Average energy consumption versus the normalized sensing duration for COV detector with various detection thresholds.

It is shown that more energy is consumed as the detection threshold increases from the bottom to the top. One can see that the energy consumption increases when the sensing duration increases for both detectors. However, if the sensing duration increases further, the consumed energy will be reduced. When $\tau_s$ is set to the smallest value as 0.001, only nearly

0.002J energy is consumed for COV when $\gamma_{COV} = 1.02$, whereas much more energy as 0.02J needs to be consumed for EG when $\gamma_{EG} = 1.005$. When $\tau_s$ reaches the maximum duration, the same energy consumption is $p_s T = 0.011$J for both detectors. One also sees that the COV detector has a longer sensing duration than the EG detector when it reaches the maximum energy consumption, as the COV detector needs more samples due to its complexity. On the other hand, the maximum energy consumption of the COV detector is smaller than that of the energy detector. For example, when the threshold is 1.025, the maximum energy consumption for the COV detector is about 0.015J with the sensing duration $\tau_s = 0.066s$, while when the threshold is 1.01, the maximum energy consumption for the EG is around 0.025J with the sensing duration $\tau_s = 0.018s$. For the same reasons, the consumed energy for the EME detector has a similar trend to that of the COV detector, namely, the energy consumption increases with the sensing duration and then decreases. The maximum energy consumption for EME is about 0.018J when $\tau_s = 0.062s$. This figure is not shown here for the compactness of the paper.

In addition to the sensing duration, the sensing threshold is also another important parameter that will affect the performance of energy-harvesting CRN. In order to observe the effect of different sensing thresholds on the energy causality constraint, collision constraint and their tradeoff separately for the three detectors, and therefore to find the optimal sensing duration under different conditions, three exclusive subsets of sensing thresholds are used based on the signal power and noise power. Consequently, the following examples illustrate the relationships between the sensing duration and the system performance corresponding to the sensing threshold.
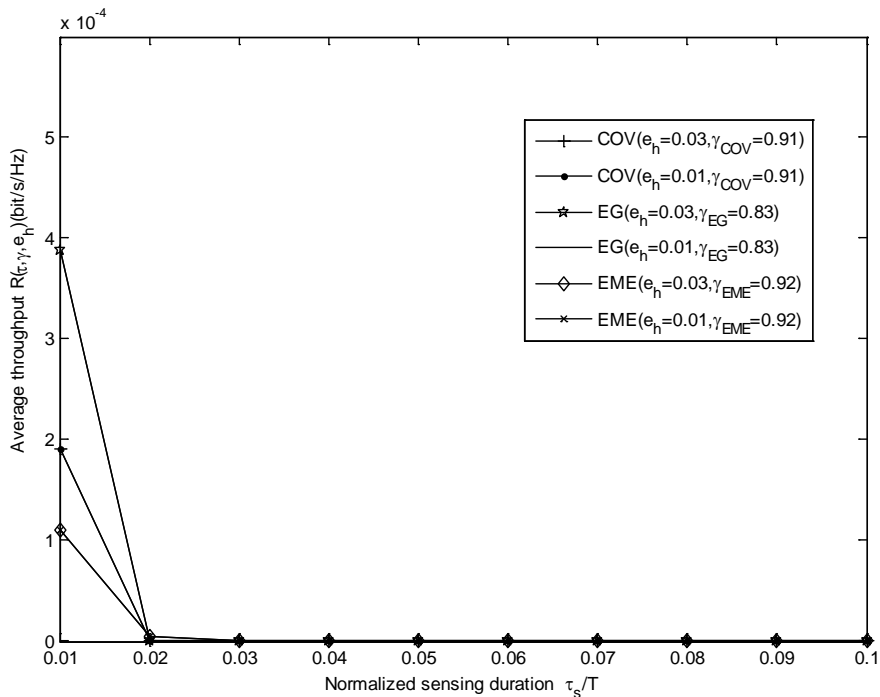


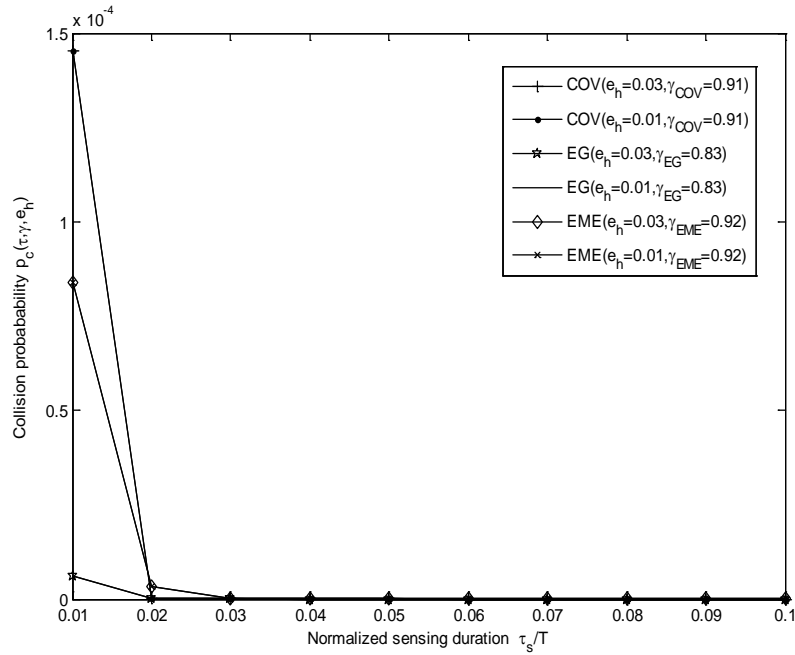**Fig. 3.** Average throughput versus the normalized sensing duration when $0 \le \gamma < \sigma_w^2$.

**Fig. 4.** Collision probability versus the normalized sensing duration when $0 \leq \gamma < \sigma_w^2$.

**Figs. 3** and **4** compare the average throughput and collision probability versus the normalized sensing duration for different detectors when the sensing threshold $0 \leq \gamma < \sigma_w^2$. Different harvested energy is also considered with respect to the same sensing threshold for any detector. In this case, as the sensing duration increases, the average throughput and collision probability are both small and monotonically decrease. Thus, there is no optimal sensing duration for the three detectors.
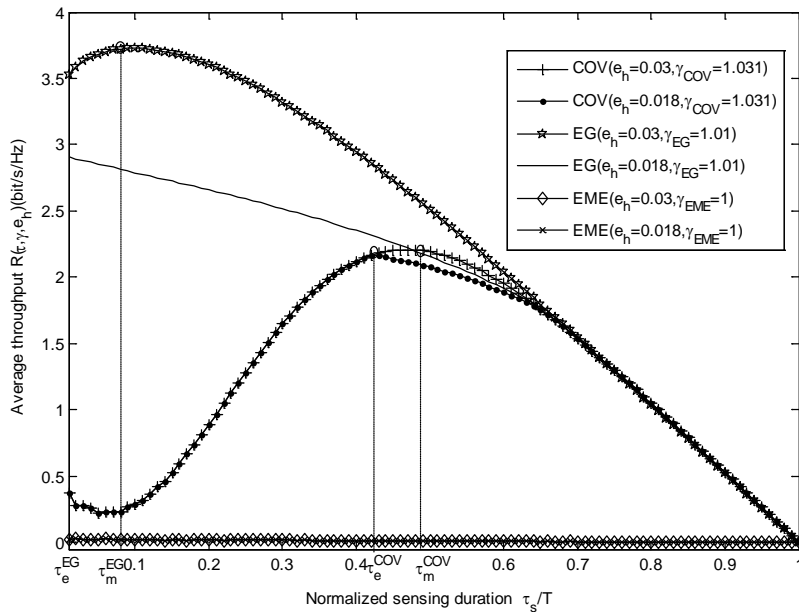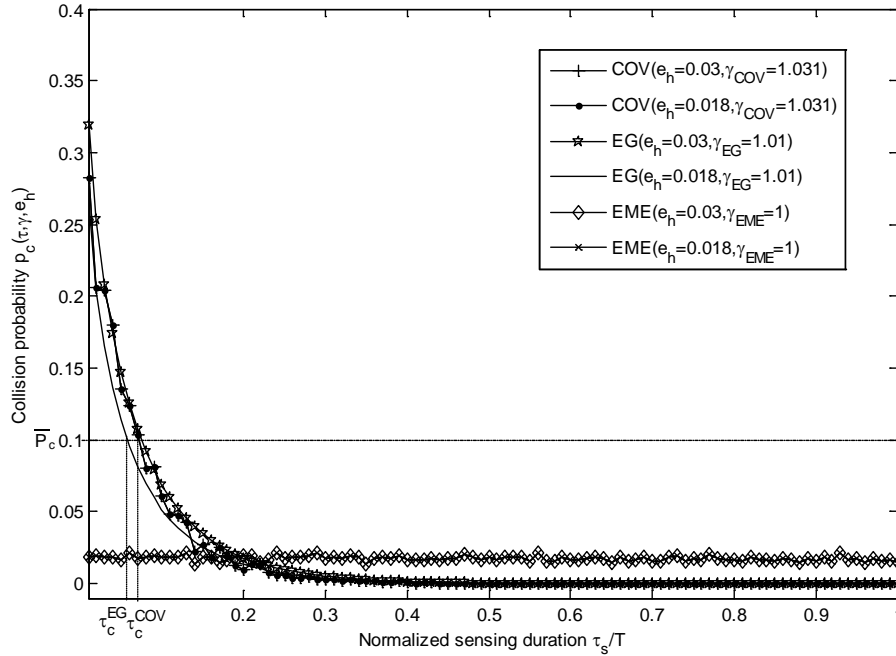


**Fig. 5.** Average throughput versus the normalized sensing duration when $\sigma_w^2 \leq \gamma < \sigma_w^2 + \sigma_p^2$.

**Fig. 6.** Collision probability versus the normalized sensing duration when $\sigma_w^2 \leq \gamma < \sigma_w^2 + \sigma_p^2$.

**Figs. 5** and **6** illustrate the average throughput and the collision probability for different detectors when the sensing threshold $\sigma_w^2 \leq \gamma < \sigma_w^2 + \sigma_p^2$. One can see that the average throughput and the collision probability decrease when the harvested energy decreases. Also, both the EG and COV detectors have a non-zero value of $\tau_m$ that maximizes the average throughput. For the same average harvested energy, a value of $\tau_c$ can be found to satisfy the collision constraint for the COV detector and the EG detector, but not for the EME detector due to its small collision probability. Furthermore, if the target collision probability $\overline{P}_c$ is set to 0.1, when the average harvested energy decreases to the same value of 0.018J, $\tau_e^{EG}$ is smaller than $\tau_c^{EG}$ for the EG detector, and $\tau_e^{COV}$ is larger than $\tau_c^{COV}$ for the COV detector. Consequently, in order to satisfy the collision constraint, the optimal sensing duration is designed to $\tau_c^{EG}$ for the EG detector and $\tau_e^{COV}$ for the COV detector, which indicates that the range of energy-equilibrium region is shorter for the EG detector than the COV detector for a given average harvested energy.

**Figs. 7** and **8** show the average throughput and the collision probability versus the normalized sensing duration for different detectors when the sensing threshold $\gamma > \sigma_w^2 + \sigma_p^2$. In this case, all three detectors can achieve the maximum throughput with a non-zero $\tau_m$. Compared with the EG detector, both the COV and the EME detectors have larger energy-equilibrium duration. As for the collision probability, it increases as the normalized sensing duration increases for all three detectors. This is because when the sensing threshold is greater than the primary signal power, so the ST considers the spectrum as being idle when it is

actually being occupied. Thus, this condition is not considered to be reasonable for practical use. This figure identifies this unreasonable condition and therefore is useful.
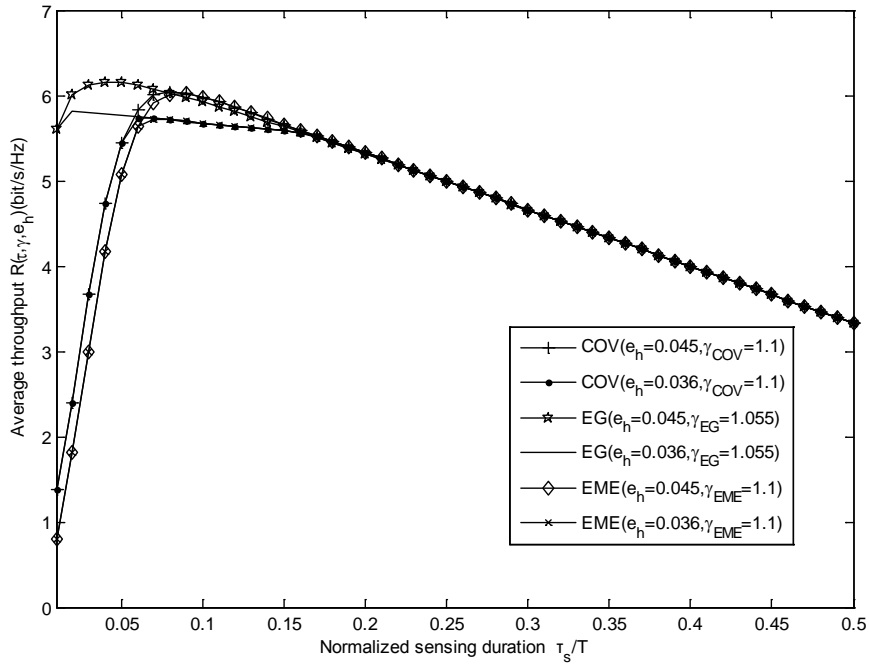


**Fig. 7.** Average throughput versus the normalized sensing duration when $\gamma > \sigma_w^2 + \sigma_p^2$.
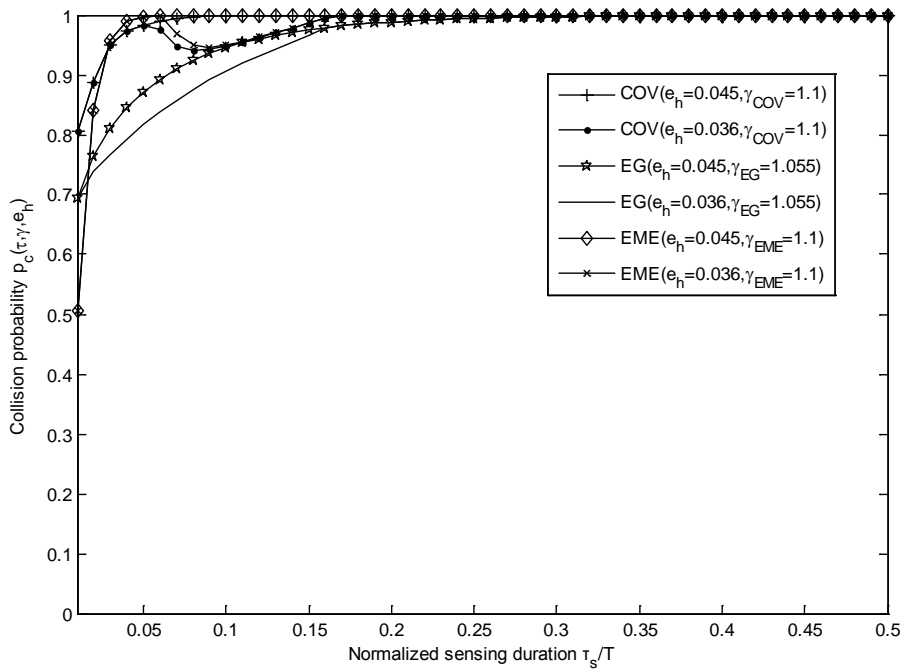


**Fig. 8.** Collision probability versus the normalized sensing duration when $\gamma > \sigma_w^2 + \sigma_p^2$.

The above discussions analyze how the value of $\gamma$ will affect the throughput performances of different detectors and compare their performances for the same value of $\gamma$. Using these discussions, one can also design the detectors by choosing the value of $\gamma$ according to the following rules. From **Figs. 1** and **2**, the threshold needs to be as large as possible to achieve larger throughput. However, when the threshold is too large, such as in Figs. 7 and 8, the condition becomes unreasonable. Thus, it is preferable to choose a value of threshold in the condition of **Figs. 5** and **6** for a practical system.

## 6. Conclusion

Two feature-based detectors have been examined and compared with the energy detector for energy harvesting CRN. Numerical examples show that the optimal sensing duration can be derived only for an appropriate sensing threshold. Compared with energy detector, there is no optimal sensing duration for the EME detector due to its poor sensing performance. However, for a reasonable sensing threshold, considering the COV detector usually outperforms the energy detector, the range of energy-equilibrium region is longer than the EG detector for a given average harvested energy.

## References

[1] Y. He, X. Cheng, W. Peng, G.L. Stuber, "A survey of energy harvesting communications: models and offline optimal policies," *IEEE Commun. Mag.*, vol. 53, no. 6, pp. 79-85, 2015. Article (CrossRef Link)

[2] X. Huang, T. Han, N. Ansari, "On green-energy-powered cognitive radio networks," *IEEE Commun. Surv. & Tut.,* vol. 17, no. 2, pp. 827 – 842, 2015. Article (CrossRef Link)

[3] H. Gao, W. Ejaz, M. Jo, "Cooperative wireless energy harvesting and spectrum sharing in 5G networks," *IEEE Access*, vol. 4, pp. 3647 – 3658, July 2016. Article (CrossRef Link)

[4] N. Zhao, F.R. Yu, V.C.M. Leung, "Opportunistic communications in interference alignment networks with wireless power transfer," *IEEE Wireless Commun.*, vol. 22, no. 1, pp. 88 – 95, 2015. Article (CrossRef Link)

[5] N. Zhao, F.R. Yu, V.C.M. Leung, "Wireless energy harvesting in interference alignment networks," *IEEE Commun. Mag.*, vol. 53, no. 6, pp. 72 – 78, 2015. Article (CrossRef Link)

[6] Z. Wang, Z. Chen, B. Xia, L. Luo, J. Zhou, "Cognitive relay networks with energy harvesting and information transfer: design, analysis, and optimization*," IEEE Trans. Wireless Commun.,* vol. 15, no. 4, pp. 2562-2576, Apr. 2016. Article (CrossRef Link)

[7] S. Park, H. Kim, and D. Hong, "Cognitive radio networks with energy harvesting," *IEEE Trans. Wireless Commun.*, vol. 12, no. 3, pp. 1386-1397, Mar. 2013 Article (CrossRef Link)

[8] W. Chung, S. Park, S. Lim, D. Hong, "Optimal transmit power control for energy-harvesting cognitive radio system," in *Proc. of Vehicular Technology Conference (VTC Fall), 2013 IEEE 78th*, pp. 1-5, 2013. Article (CrossRef Link)

[9] J. Jeya Pradha, S. S Kalamkar, A. Banerjee, "Energy harvesting cognitive radio with Channel-Aware Sensing Strategy," *IEEE Commun. Lett.*, vol.18, no.7, pp.1171-1174, Jul. 2014. Article (CrossRef Link)

[10] A. Sultan, "Sensing and transmit energy optimization for an energy harvesting cognitive radio," *IEEE Wireless. Commun. Lett.*, vol.1, no.5, pp.500-503, Oct. 2012. Article (CrossRef Link)

[11] M. López-Benítez, F. Casadevall, "Signal uncertainty in spectrum sensing for cognitive radio," *IEEE Trans. Commun.*, vol. 61, no.4, pp.1231-1241, Apr. 2013. Article (CrossRef Link)

[12] Y. Zeng, C. L. Koh, and Y.-C. Liang, "Maximum eigenvalue detection: theory and application," in *Proc. of IEEE Int. Conf. Communications (ICC'08)*, Beijing, China, pp.4160-4164, May 2008. Article (CrossRef Link)

[13] Y. Zeng and Y.-C. Liang, "Eigenvalue-based spectrum sensing algorithms for cognitive radio," *IEEE Trans. Commun*., vol.57, no. 6, pp. 1784-1793, Jun. 2009. Article (CrossRef Link)

[14] Y. Zeng and Y.-C. Liang, "Covariance based signal detections for cognitive radio," in *Proc. of DySPAN2007*, Dublin, Ireland, pp. 202-207, Apr.2007. Article (CrossRef Link)

[15] Y. Chen, C. Wang and B. Zhao, "Performance comparison of feature- based detectors for spectrum sensing in the presence of primary user traffic," *IEEE Signal Processing Letters*., vol. 18, no.5, pp. 291-294, May. 2011. Article (CrossRef Link)

**Yan Gao** received her M.E. degree in Signal and Information Processing from Yangzhou University, Yangzhou, P. R. China, in June 2006. She is currently working at School of Electronic Information, Nanjing College of Information Technology. Her current research interests include wireless energy harvesting, cognitive radio and signal processing in communication.

**Yunfei Chen** is an Associate Professor in the School of Engineering at the University of Warwick, Coventry, UK. He received his B.E. and M.E. degrees from Shanghai Jiaotong University, Shanghai, China, in 1998 and 2001, respectively. He received his Ph.D. degree from University of Alberta, Canada, in 2006. His current research interests include cognitive radios, energy harvesting, wireless relaying and performance analysis.

**Zhibin Xie** received the M.E. degree in Pattern Recognition and Intelligent Systems in 2007, and the Ph.D. degree in Communication and Information Systems, from Northeastern University, Shenyang, P. R. China, in 2009. He is currently working at School of Information and Electronic Engineering, Jiangsu University of Science and Technology. His current research interests include green communication, cognitive radio and heterogeneous networks.

**Guobing Hu** is a vice professor of School of Electronic Information Engineering and the Director of Research Center of Information Cogition and Intelligent Compuation, Jinling insititue of Technology, Nanjing, P. R. China. He received his PhD degree in Communication and Information System from Nanjing University of Aeronautics and Astronautics, in 2011. His current research interests include signal processing in communication, cognitive radio.